Metal-Quinoid Carbene Chemistry. From Bonding to C–H Activation Catalysis

Hai-Xu Wang[a]
Kai Wu[a]
Chi-Ming Che*[a,b]

[a] State Key Laboratory for Synthetic Chemistry, Department of Chemistry, The University of Hong Kong, Pofkulam Road, Hong Kong, China.

[b] HKU Shenzhen Institute of Research & Innovation, Shenzhen, 518053, China.

cmche@hku.hk

Click here to insert a dedication.

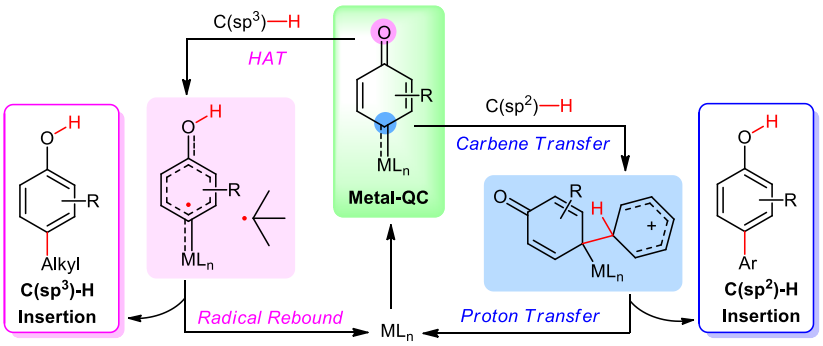

Received:
Accepted:
Published online:
DOI:

Abstract This account summarizes our recent works on metal-quinoid carbene (QC) chemistry including (1) $[Rh_2(esp)_2]$-catalyzed QC C(sp^2)–H insertion reaction enabled by a C-centered carbene transfer reactivity, (2) isolation, characterization, and dual reactivity feature of Ru(II) porphyrin QC complexes, and (3) Ir(III) porphyrin-catalyzed QC C(sp^3)–H insertion reaction initiated by an O-centered hydrogen atom transfer (HAT) reactivity of metal-QC species.

1 Introduction
2 Catalytic QC Insertion into C(sp^2)–H Bonds Enabled by Carbene Transfer Reactivity
3 Ru(II) Porphyrin QC Complexes and Dual Reactivity
4 Catalytic QC Insertion into C(sp^3)–H Bonds Enabled by HAT Reactivity
5 Perspective and Outlook

Key words metal carbene chemistry – homogeneous catalysis – C–H functionalization – arylation – redox-noninnocent ligand – hydrogen atom transfer

1 Introduction

Metal-quinoid carbene (QC) species, which can be regarded as replacing one of the oxygen atoms in an organic quinone by a metal atom/ion (Scheme 1a), are a promising yet underdeveloped class of reactive species for carbene transfer and insertion reactions.[1] Different from other reactive carbene groups (e.g., acceptor carbenes, donor-acceptor carbenes) which generally act as alkyl synthons, metal-QC species can act as aryl synthons since after the initial transfer/insertion step, the carbene groups can undergo aromatization to give functionalized phenol moieties. Although early works on transition metal-catalyzed QC transfer reactions have been reported in the late 1980s, it is not until the last decade that a growing interest has been dedicated to this field,[2] and up to now, cyclopropanation,[3] C(sp^2)–H insertion,[4] C(sp^3)–H insertion,[4k,5] X–H insertion,[5a,6] and other C–C and C–X bond formation reactions[6-7] have been developed (Scheme 1a). Despite these advances, the electronic structure and reactivity of the plausible metal-QC intermediates which have not been isolated or spectroscopically detected remain elusive. Previously, only two examples of metal-QC complexes, a Ru and an Fe complex (also termed as ruthenaquinone and ferraquinone), have been reported in the literature,[8] both of which are stabilized by chelating phosphine ligands but have not been reported to display carbene transfer

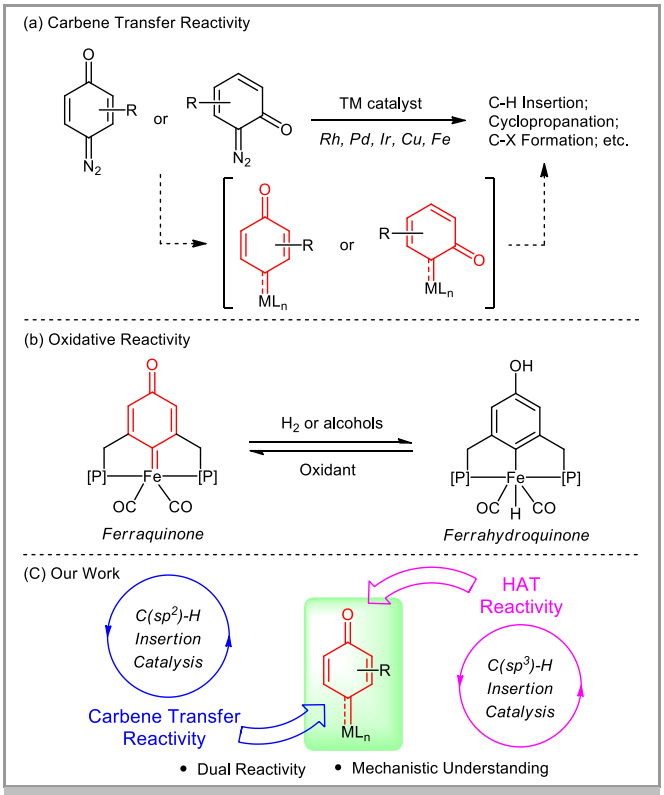

Scheme 1 Literature reports on the carbene transfer reactivity (a) and oxidative reactivity (b) of metal-QC species. (c) Summary of our works in this account

and insertion reactivity. Interestingly, the ferraquinone complex could undergo a formal 1,6-addition with H_2, HCl, and alcohols (Scheme 1b).[8b] However, no crystal structures of these metal-QC complexes in a quinoid form were obtained.

In this account, we present our recent works on metal-QC chemistry (Scheme 1c), with particular foci on the understanding of reactive QC intermediates and also on how the understanding helps in the development of new catalytic methodologies. Firstly, a [Rh_2(esp)$_2$]-catalyzed intermolecular QC C(sp^2)–H insertion reaction via a canonical carbene transfer mechanism is described.[9] Secondly, a series of stable Ru(II) porphyrin QC complexes have been isolated and characterized (including X-ray crystallography), and these complexes exhibit dual reactivity feature, i.e., a C-centered 2e$^-$ carbene transfer reactivity and an O-centered 1e$^-$ hydrogen atom transfer (HAT) reactivity.[10] Lastly, the HAT reactivity of metal-QC complexes has led us to design an Ir(III)-catalyzed intermolecular QC C(sp^3)–H insertion reaction passing through a unique radical pathway which is less common in catalytic C–H functionalization reactions by metal-carbene species.[11]

2 Catalytic QC Insertion into C(sp^2)–H Bonds Enabled by Carbene Transfer Reactivity

Previously, Rh_2(II,II) carboxylate catalysts were reported to catalyze the transfer of QC groups onto alkenes[3a-c, 4a] and enol ethers,[7c] and insertion into C–H bonds,[4b, 5b] O–H bonds,[5a] and alkyl halides;[7e] the synthetic utility of some of these reactions have been demonstrated by Baran[3c] and others[3a,b] in the preparation of natural products and bioactive molecules. Insertion of QC into C(sp^2)–H bonds affording biaryl coupling product is another promising methodology as it circumvents the use of prefunctionalized aryl substrate which is required in traditional biaryl coupling reactions. Such a transformation has been achieved with directing group (DG)-containing substrates,[4d-g,i,j] yet installation/removal of DGs would reduce the atom-economy and limit the substrate scope. We envisioned that, by harnessing the high electrophilicity of the Rh-QC intermediates, biaryl products could be obtained by using DG-free arenes as nucleophilic substrates via direct QC C(sp^2)–H insertion (Scheme 2a). Although similar reactions have been reported before,[4b,c,h] they are either intramolecular reactions or suffer from limited scope of arene/QC partner. An intermolecular reaction between simple and readily available arenes as well as a wide scope of QCs, including both p- and o-quinone diazides, is therefore highly desirable. With [Rh_2(esp)$_2$] as the catalyst and anisole as a nucleophilic C(sp^2)–H substrate, the insertion product 1a could be obtained in high yield with high regioselectivity (> 20:1) at the para position.[9] [Rh_2(esp)$_2$] showed superior activity to [Rh_2(OAc)$_4$] and other common carbene transfer catalysts (Table 1). The plausible Rh-QC intermediate was computed to adopt a quinoid form with a Rh–$C_{carbene}$ distance of 1.980 Å (Scheme 2b). An important piece of mechanistic information is the kinetic isotope effect (KIE). By using anisole/anisole-d_5 as substrates, an inverse KIE value of ca. 0.87 was obtained (Scheme 2e), and such a secondary KIE supports the nucleophilic addition of anisole to the carbene carbon atom as a rate-determining step since it involves an sp^2-to-sp^3 rehybridization. This is corroborated by DFT calculations (Scheme 2d) suggesting a relatively high barrier for nucleophilic attack (11.8 kcal mol^{-1}), and the C–H bond is cleaved in the subsequent rearomatization step via proton transfer with a relatively low barrier (3.5 kcal mol^{-1}). As depicted in Scheme 2c, the TS structure of nucleophilic attack (TS1) features a QC group that is bent yet still σ-bonded to Rh.

Table 1 Reaction Optimization (Selected)[a]

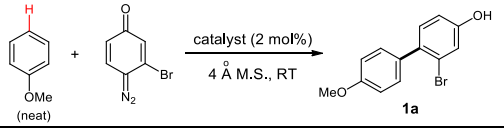

Entry	Catalyst	Conv. (%)	Yield of **1a** (%)
1	[Rh_2(esp)$_2$]	100	87
2	[Rh_2(OAc)$_4$]	100	14
3	[Cu(CH$_3$CN)$_4$(PF$_6$)]	51	8
4	[Co(TTP)]	44	17
5	[Ru(TTP)(CO)]	9	36
6	[Ir(TTP)Me]	100	0
7	[(Ph$_3$P)AuCl]/AgSbF$_6$	14	7

[a] See ref 9 for more details in reaction optimization

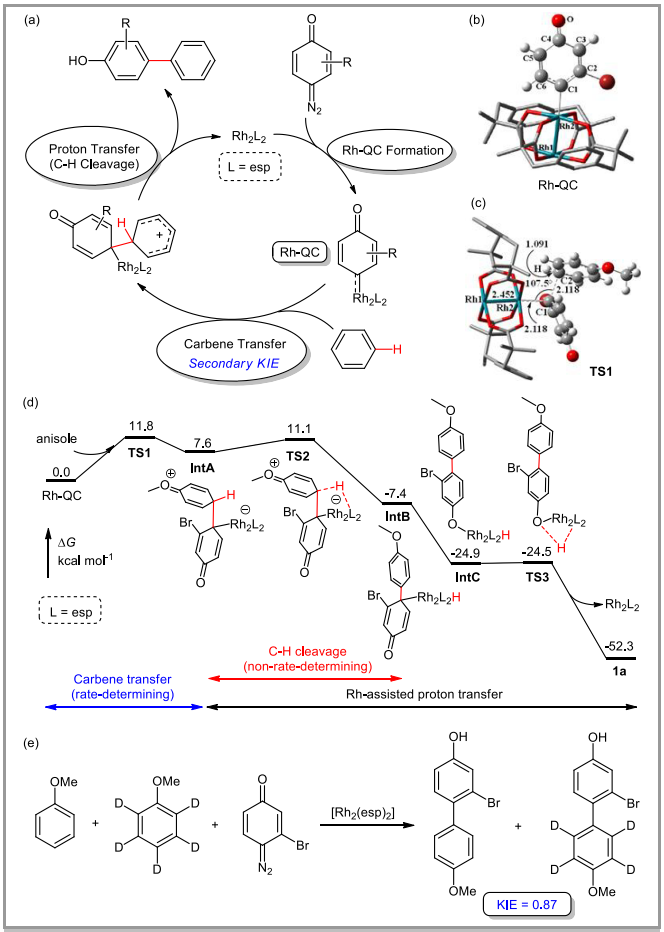

Scheme 2 (a) Proposed catalytic cycle of the Rh_2(II,II)-catalyzed QC C(sp^2)–H insertion reaction. (b) Calculated structure of the Rh-QC intermediate. (c) Calculated TS structure of the carbene transfer step **TS1**. (d) Secondary KIE determined by anisole/anisole-d_5

This method can be extended to a number of simple arenes and electron-rich hetereoarenes, as well as substituted p- and o-quinone diazides, providing direct access to biaryl products (Scheme 3). Regioselectivity is controlled by both electronics and sterics. Insertion of Rh-QC intermediates into arene substrates follows the sequence of para > ortho > meta (1a,b in Scheme 3), and high r.r. (> 16:1) could be achieved with electron-rich arenes. Electron-deficient arenes (e.g., PhBr, PhF) can also be arylated,

albeit with decreased yield and selectivity. While insertion into pyrrole occurs at the more electron-rich C2 position, reactivity can be tuned to the C3 position when a bulky substituent is present on the pyrrolic nitrogen (1c,d in Scheme 3). Synthetic application of this protocol has been demonstrated by the late-stage functionalization of drugs and functional materials (1e–g in Scheme 3); it can also be used to prepare a bioactive compound, transthyretin amyloid inhibitor (1i, inset of Scheme 3), in a simple two-step synthesis.

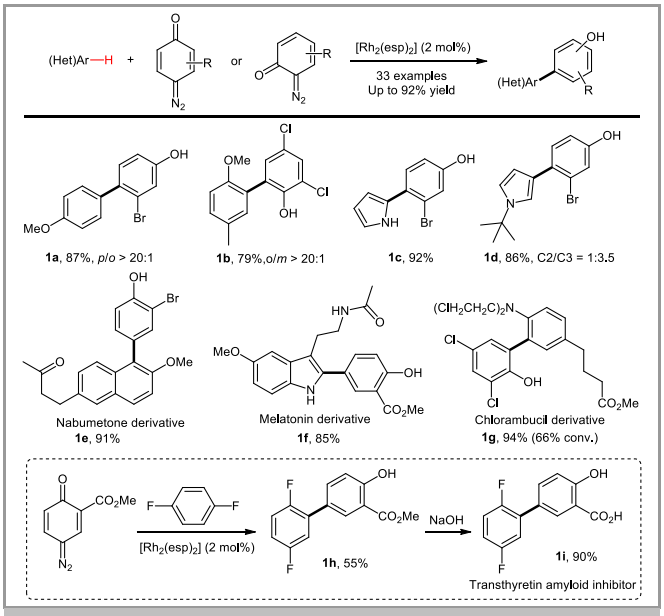

Scheme 3 Selected substrate scope of catalytic QC C(sp²)–H insertion reaction. See ref 9 for the full substrate scope and detailed experimental conditions

3 Ru(II) Porphyrin QC Complexes and Dual Reactivity

Our previous work showed that the quinoid form of a metal-QC intermediate is likely responsible for the carbene transfer reactivity. In the literature, it has been reported that the quinoid form of ruthenaquinone complex easily underwent tautomerization to its aromatic form, e.g., during crystallization process;[8a] no crystal structure of metal-QC complexes in a quinoid form has been reported before. To address this issue, we turned to Ru(II) porphyrin system which is well-known for stabilizing a variety of Ru-carbene units,[12] including those of acceptor-acceptor, donor-acceptor, and acceptor carbenes. Ru-carbene complexes are generally prepared from [Ru(Por)(CO)] and the corresponding diazo precursors. Similarly, the Ru porphyrin QC complexes [Ru(Por)(QC)] (Por = porphyrinato dianion) can also be readily synthesized from [Ru(Por)(CO)] and the diazo compounds of QCs, i.e., quinone diazides (Scheme 4a).[10] The carbene ligands of these [Ru(Por)(QC)] complexes are in the quinoid form in the solid state according to X-ray crystal structures (Scheme 4b) and IR spectroscopy. Solvatochroism of the ruthenaquinone complex was previously observed and attributed to the tautomerization between a quinoid form and an aromatic form. However, [Ru(Por)(QC)] complexes are stable in either nonpolar or polar solvents, and their quinoid form in the solution state is corroborated by ^{13}C NMR where two low-field signals assignable to Ru=C and C=O have been observed for each complex. Cyclic voltammetry revealed the redox-noninnocent feature of QC ligands as the Ru-QC complexes display two reversible reduction waves, and the reduction potentials of QC ligands (–1.26 ~ –0.67 V vs $Fc^{+/0}$ in dichloromethane, same as below) are comparable to that of organic quinones (ca. –1 V). The first oxidation (0.28–0.54 V) is ascribed to be porphyrin-centered based on UV-vis spectroelectrochemistry, from which the π-acidity of QC ligands could be inferred to be comparable to and even stronger than a carbonyl ligand (0.32 V for [Ru(TMP)(CO)]); by contrast, a Ru(III/II) couple is observed as the first oxidation event for Ru porphyrins bearing phenyl-/ester-substituted carbene ligands.[12f,j] This can also rationalize the lack of a quinoid-aromatic tautomerization since the QC ligands are not capable of oxidizing the Ru(II) centers in Ru-QC complexes, whereas in the previous ruthenaquinone complex, a formally Ru(0) center might be reducing enough to induce such a tautomerization.[8a] In addition to the above spectroscopic characterizations, the electronic structure of [Ru(Por)(QC)] has further been studied by DFT calculations. Different from many metal-carbene species in which the carbene π^* orbitals are mainly localized at the carbene carbons, Ru-QC complexes feature a unique delocalized and low-lying carbene π^* orbital throughout the whole QC plane (Scheme 4c). We conceive that this delocalization is crucial for the dual reactivities of Ru-QC complexes taking place at both carbene carbon (C-centered) and carbonyl oxygen (O-centered) as discussed below.

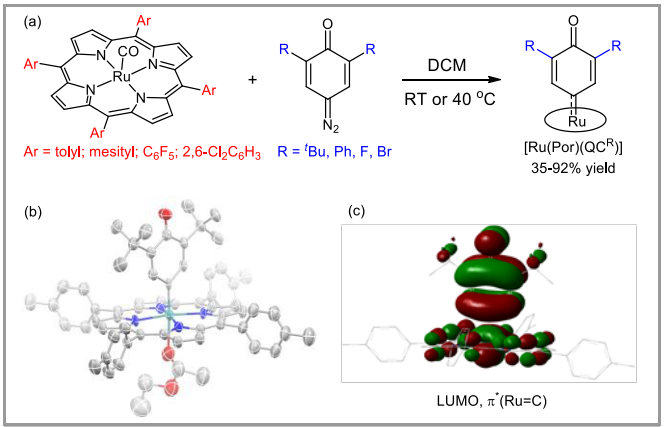

Scheme 4 (a) Synthesis of [Ru(Por)(QC^R)] complexes. (b) Crystal structure of [Ru(TTP)(QC^{tBu})(AcOEt)]. (c) Calculated QC π^* orbital of [Ru(TTP)(QC^{tBu})].

[Ru(Por)(QC)] complexes can undergo stoichiometric carbene transfer reactions with nitrosoarenes (ArNO) to give nitrone compounds in high yields (Scheme 5a); such a transformation has been regarded as a key step in the previous examples of Ru porphyrin-catalyzed three component coupling reactions of diazo compound, ArNO, and dipolarophiles.[13] The corresponding [Ru(Por)(CO)]-catalyzed nitrone formation reaction from quinone diazide and ArNO can also be developed, albeit with only moderate product yields. The stoichiometric reaction was first-order to both [Ru(Por)(QC)] and ArNO, and no apparent induction period could be observed, both suggesting that the five-coordinate [Ru(Por)(QC)] complexes are directly reactive toward ArNO without the need of activation by a sixth axial ligand.[12i, 14] This is further supported by DFT calculations as well as by the finding that no binding between [Ru(Por)(QC)] and ArNO could be detected by UV-vis titration experiment. Hammett studies on the reactivity of [Ru(Por)(QC)] and ArNO revealed some intriguing features. While a negative ρ value characteristic

of a nucleophile was found for ArNO, the ρ value for substituents on the QC ligands was also negative (Scheme 5b), which leads to a counterintuitive conclusion that an electron-donating substituent can enhance the reactivity of an electrophilic carbene group. Furthermore, a similar negative ρ value was also found for QC substituent in the catalytic nitrone formation reaction. To explain this reverse carbene substituent effect, computational studies have been performed to compare the transition states (TSs) of the most active [Ru(TTP)(QC^{tBu})] and the least reactive [Ru(TTP)(QC^{Br})]. The calculated rate constants could well reproduce the experimental data, and the kinetic barrier of [Ru(TTP)(QC^{tBu})] is ca. 1 kcal mol^{-1} lower in energy than that of [Ru(TTP)(QC^{Br})]. Early TSs were found for both species, in which the QC planes are significantly bent while still σ-bonded to the Ru centers. Both TSs are highly similar in structure, and the most distinct difference between them is the bending angle of the QC plane, as the more reactive QC^{tBu} group bends ca. 10° less than the less reactive QC^{Br} group, which we conceive to account for the ca. 1 kcal mol^{-1} energy difference (Scheme 5c). A mechanistic model has been proposed as follow: in such an early TS, the major event taking place is the breaking of the metal-carbene π bond; since QC ligand with a more electron-donating substituent is less π-accepting and forms a weaker π bond with the Ru center, a smaller distortion is needed to break the Ru–C$_{carbene}$ π bond and thus a lower energy barrier to reach the TS. Other factors potentially contributing to the kinetic barrier such as electrostatics and sterics can be precluded since only negligible differences in these factors have been found between [Ru(TTP)(QC^{tBu})] and [Ru(TTP)(QC^{Br})]. In summary, this is the first example of metal-QC species capable of undergoing carbene transfer reactions.

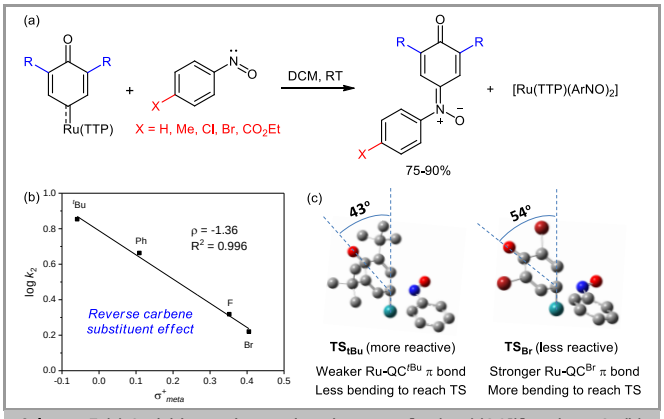

Scheme 5 (a) Stoichiometric reactions between [Ru(TTP)(QC^{R})] and ArNO. (b) Hammett study on the carbene substituent R (R = ^{t}Bu, Ph, F, Br). (c) Transition state structures derived from [Ru(TTP)(QC^{tBu})] (**TS1$_{tBu}$**) and [Ru(TTP)(QC^{Br})] (**TS1$_{Br}$**)

The O-centered HAT reactivity of [Ru(Por)(QC)] complexes is discovered serendipitously. During the investigation of potential C(sp^3)–H insertion reactivity of [Ru(Por)(QC)] by using 1,4-cyclohexadiene as substrate, the oxidized benzene product was obtained in high yield, along with a Ru(III)-aryl product which is likely formed via HAT and redox-induced electron transfer (RIET)[15] from the Ru(II) center to the QC ligand (Scheme 6a). The Ru(III)-aryl species could be readily oxidized back to the Ru(II)-QC complex, thereby forming a 1H$^+$/1e$^-$ couple reminiscent of the organic quinone/semiquinone couple; it is noteworthy that the previous ferraquinone/ferrahydroquinone redox couple involves a 2H$^+$/2e$^-$ process similar to the organic quinone/hydroquinone couple (Scheme 1b).[8b] By making use of such a redox couple, an aerobic oxidation reaction catalyzed by the Ru(II)-QC complex could be developed with a turnover number of up to 48. The HAT mechanism is corroborated by a primary KIE of ca. 6.6 with 9,10-dihydroanthracene(DHA)/DHA-d$_4$ as substrates (Scheme 6b), and also by activation parameters including a negative activation entropy suggestive of an associative HAT step (Scheme 6c). Lewis acid effect and porphyrin effect further support that the HAT reactivity is O-centered rather than C-centered. The proposed HAT and RIET may occur concomitantly as only one TS could be found by DFT calculations, in which the aromaticity of QC moiety is midway between those in the Ru(II)-QC and in the Ru(III)-aryl species. Such a HAT reactivity is unprecedented for metal-carbene complexes to the best of our knowledge, and is closely related to the low-lying and delocalized carbene π* orbitals which is unique to metal-QC species.

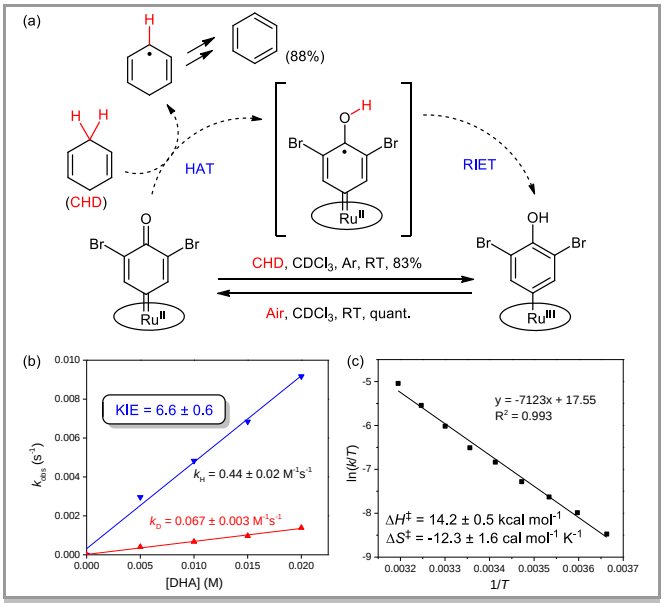

Scheme 6 (a) Stoichiometric HAT reactivity of [Ru(Por)(QC^{Br})]. (b) Primary KIE measured with DHA/DHA-d$_4$. (c) Activation parameters determined by Eyring plot

4 Catalytic QC Insertion into C(sp^3)–H Bonds Enabled by HAT Reactivity

QC C(sp^3)–H insertion is another appealing strategy since it allows direct arylation of C(sp^3)–H bonds. Nevertheless, the mechanism for C(sp^2)–H insertion described in Section 2 is barely applicable to C(sp^3)–H bonds given the low nucleophilicity of saturated hydrocarbons, though it might still be operative for a few intramolecular reactions.[5] On the other hand, the HAT reactivity of Ru(II)-QC complexes offers the possibility of a stepwise C(sp^3)–H insertion process via HAT followed by radical rebound, which resembles that of metal-oxo species. In the system of Ru(II)-QC, formation of the Ru(III)-aryl product as a thermodynamic sink prohibits the subsequent rebound step, and the alkyl radical generated by HAT is simply oxidized to arene/ketone. An electrophilic and less reducing metal center could likely promote rebound reactivity due to increased radical character of the QC ligand. After initial screening we discovered that Ir(III) porphyrins are highly efficient catalysts for the QC

C(sp³)–H insertion reactions with quinone diazides as QC sources (Table 2),[11] and this is reasonable since Ir(III) is barely reducing and Ir(IV) porphyrin/porphyrinoid species have only been detected spectroscopically and never been isolated.[16] Detailed mechanistic studies on all elementary steps and reaction intermediates were conducted to support such a radical mechanism (Scheme 7a) since it is not common for carbene C(sp³)–H insertion reactions.[17] The first elementary step is decomposition of quinone diazide to form the Ir-QC intermediate, which has been characterized by ^{1}H NMR and mass spectroscopy; formation of the azine product in the absence of aliphatic substrate also infers the existence of Ir-QC species since azine formation has been observed for reactive metal-carbene species in the presence of excess diazo compounds.[18] DFT calculations on the Ir-QC intermediate reveal a very similar electronic structure to the Ru(II) analogue including a characteristic low-lying and delocalized carbene π^* orbital. The second elementary step is HAT, and a primary KIE value of ca. 3.2 has been determined with THF/THF-d_8 as substrates (Scheme 7c). Radical trapping experiments with TEMPO strongly support the intermediacy of alkyl radical, and steric control experiments are in favor of an O-centered HAT process. The crucial Ir-QC-H· intermediate has been characterized by EPR, and the anisotropic signals ($g_\perp$ = 2.055 and $g_\parallel$ = 1.961) suggest the presence of Ir-centered spin density (resonance form B); however, these signals are less anisotropic (especially the $g_\parallel$ component) than authentic Ir(IV) salen complexes (g_x, g_y = 2.10–2.17 and g_z = 1.51–1.55) which adopt a similar geometry, indicating significant contribution of QC ligand-radical form (resonance form A) to the electronic structure of the Ir-QC-H· intermediate (Scheme 7b). DFT calculations complied with EPR data, since major spin density was calculated to be located at the QC ligand (40%) rather than at the Ir center (20%); for the QC ligand, 75% of the spin density is localized at the carbene carbon, which could promote radical rebound to occur at the carbene carbon. The final rebound step also has a nontrivial kinetic barrier which is likely caused by the steric effect of the porphyrin ligand,[12j] as suggested by catalyst (including porphyrin ligand) screening, substrate scope study, and the aforementioned steric control experiments.

Catalyst efficiency is significantly affected by the steric environment of the porphyrin ligand. While bulky porphyrins generally retarded the reaction, the use of non-bulky OEP ligand that is free of porphyrin meso-substituents (Scheme 8) gave much improved product yield. Substrate scope was then studied with [Ir(OEP)Me] as the catalyst. Substituents on quinone diazides with various electronic properties can be well tolerated. Aliphatic substrates containing doubly activated C(sp³)–H bonds could readily undergo QC insertion with moderate to excellent product yields (Scheme 8, 2a–f), though 10 equiv of the aliphatic substrate was needed. For less activated substrates, more forcing conditions (50 °C; neat) were required to achieve satisfactory to moderate yields (2g–j). The high sensitivity of this reaction to steric factor results in the following intriguing features in regioselectivity: 1) for substituted 1,4-cyclohexadienes, high regioselectivity could be observed even with a small Me or OMe substituent (2d,e in Scheme 8); 2) for the 1-cyclohexene substrate, primary insertion was favored over insertion into other secondary C–H bonds (inset of Scheme 8); 3) for 3-

Table 2 Reaction Optimization (Selected)[a]

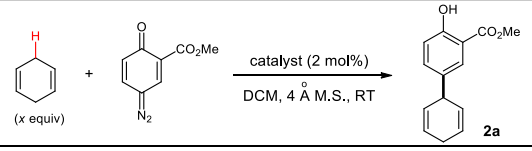

Entry	Catalyst	x (equiv)	Yield of **2a** (%)
1	[Ir(OEP)Me]	5	62
2	[$Rh_2(esp)_2$]	5	5
3	[$Cu(CH_3CN)_4(BF_4)$]	5	<1
4	[Co(TTP)]	5	<1
5	[Ru(TTP)(CO)]	5	<1
6	[Fe(TTP)Cl]	5	<1
7	[Ir(OEP)Me]	10	86

[a] See ref 11 for more details in reaction optimization

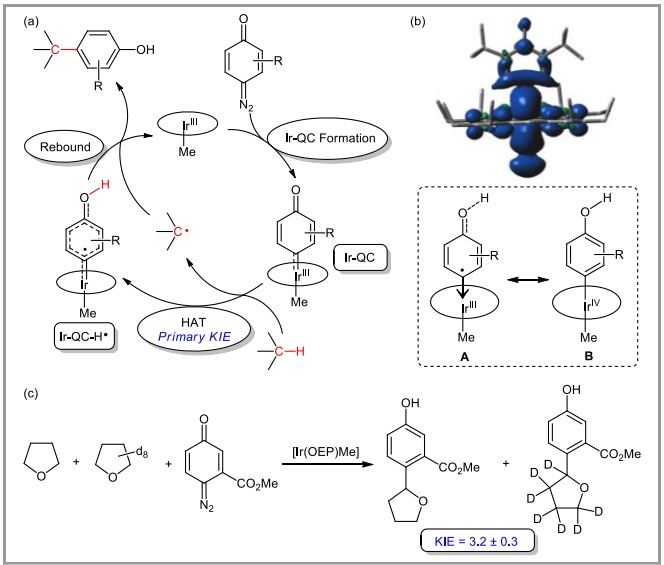

Scheme 7 (a) Proposed catalytic cycle and mechanistic studies of the Ir(III)-catalyzed QC C(sp³)–H insertion reaction. (b) Calculated spin density and proposed resonance structures of Ir-QC-H· intermediate. (c) Primary KIE determined with THF/THF-d_8

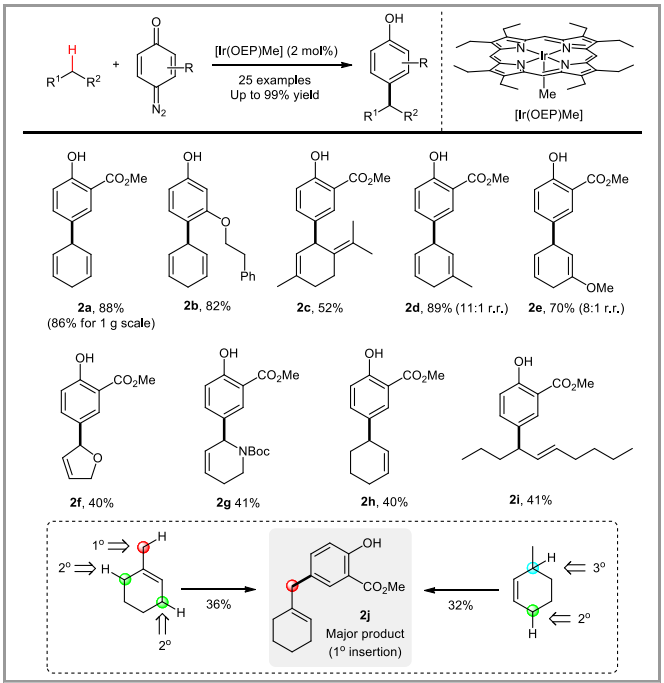

Scheme 8 Selected substrate scope of catalytic QC C(sp³)–H insertion reaction. See ref 11 for the full substrate scope and detailed experimental conditions

cyclohexene substrate which contains reactive secondary and tertiary C–H bonds, primary insertion product 2j was obtained as the major product (inset of Scheme 8), which supports our proposed radical mechanism and infers that the radical rebound step is slower than the isomerization of alkenes. Potential synthetic utility of this reaction is further demonstrated by gram-scale synthesis (2a in Scheme 8) and product transformations.

5 Perspective and Outlook

Our works have provided fundamental understanding on the dual reactivity of metal-QC species, and both reactivities can be elevated and developed into C–H activation catalysis by changing the metal and/or ligand environment (Scheme 9). Nevertheless, at this stage, catalytic QC C–H insertion reactions are still not practical enough for real synthetic applications, and the current major challenges are: 1) to make C–H substrates as limiting reagents, 2) to activate more inert C–H bonds such as light alkanes, 3) to improve efficiency and regioselectivity in complex substrate molecules, and 4) to achieve enantioselective C–H insertion reactions. Another intrinsic issue is that, after C–H insertion, the QC group will generally rearrange to phenol which contains a reactive O–H moiety, and attention has to be paid to deal with this O–H bond, either to suppress or utilize its reactivity. Based on our initial success, we conceive that some of the above challenges may be overcome by using different catalytic systems, and an appealing approach would be biocatalysis given its high efficiency and selectivity in many carbene transfer reactions. The HAT reactivity of metal-QC species also opens up new opportunities in coupling with other radical reactions including photocatalysis, electrocatalysis, and other radical cascade transformations. The use of quinone diazides as arylating reagents also merits further investigations, and very recently we have discovered a metal-free C(sp^2)–C(sp^2) bond formation reaction via cross coupling of quinone diazides and alkenyl/aryl boronic esters.[19]

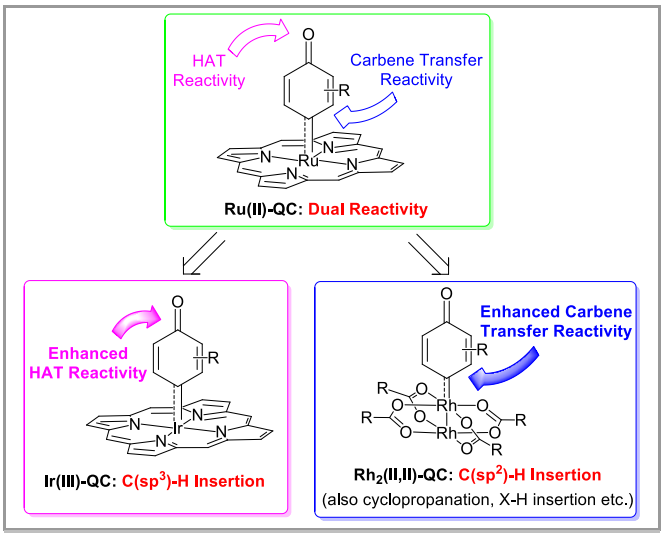

Scheme 9 Comparison of reactivity among Ru(II)-, Ir(III)-, and Rh_2(II,II)-QC species discussed in this account

Another inspiration lies in expanding the breadth of metal-carbene species, as changing the carbene substituents not only brings new functionalities to the product molecules, but may also lead to new mechanism and ultimately to new reactivity in metal carbene chemistry. In metal-QC species, the co-planarity of the carbene group plays a pivotal role in the multi-site dual reactivity as this gives rise to a conjugated and low-lying carbene π^* orbital. A quick extrapolation of this notion would land on other carbocyclic metal-carbene species whose reactivity and/or catalytic property remain underdeveloped.[20]

Funding Information

This work is supported by Hong Kong Research Grants Council (HKU 17303815) and Basic Research Program-Shenzhen Fund (JCYJ20170412140251576, JCYJ20170818141858021, and JCYJ20180508162429786).

Acknowledgment

We thank Prof. Cong-Ying Zhou, Dr. Jie-Sheng Huang, and other co-workers for their contributions to the project of metal-quinoid carbene chemistry.

References

(1) For reviews on catalytic carbene transfer/insertion reactions, see: (a) Doyle, M. P.; McKervey, M. A.; Ye, T., Modern Catalytic Methods for Organic Synthesis with Diazo Compounds. Wiley: 1998. (b) Davies, H. M. L.; Beckwith, R. E. J. Chem. Rev. 2003, 103, 2861. (c) Doyle, M. P.; Duffy, R.; Ratnikov, M.; Zhou, L. Chem. Rev. 2010, 110, 704. (d) Caballero, A.; Díaz-Requejo, M. M.; Fructos, M. R.; Olmos, A.; Urbano, J.; Pérez, P. J. Dalton Trans. 2015, 44, 20295. (e) Ford, A.; Miel, H.; Ring, A.; Slattery, C. N.; Maguire, A. R.; McKervey, M. A. Chem. Rev. 2015, 115, 9981.

(2) For a review, see: Othman, D. I. A.; Kitamura, M. Heterocycles 2016, 92, 1761.

(3) (a) Sundberg, R. J.; Baxter, E. W.; Pitts, W. J.; Ahmed-Schofield, R.; Nishiguchi, T. J. Org. Chem. 1988, 53, 5097. (b) Boger, D. L.; Jenkins, T. J. J. Am. Chem. Soc. 1996, 118, 8860. (c) Dao, H. T.; Baran, P. S. Angew. Chem. Int. Ed. 2014, 53, 14382. (d) Sundberg, R. J.; Pitts, W. J. J. Org. Chem. 1991, 56, 3048.

(4) (a) Sawada, T.; Fuerst, D. E.; Wood, J. L. Tetrahedron Lett. 2003, 44, 4919. (b) Baral, E. R.; Lee, Y. R.; Kim, S. H. Adv. Synth. Catal. 2015, 357, 2883. (c) Kitamura, M.; Takahashi, S.; Okauchi, T. J. Org. Chem. 2015, 80, 8406. (d) Zhang, S.-S.; Jiang, C.-Y.; Wu, J.-Q.; Liu, X.-G.; Li, Q.; Huang, Z.-S.; Li, D.; Wang, H. Chem. Commun. 2015, 51, 10240. (e) Chen, R.; Cui, S. Org. Lett. 2017, 19, 4002. (f) Das, D.; Poddar, P.; Maity, S.; Samanta, R. J. Org. Chem. 2017, 82, 3612. (g) Liu, Z.; Wu, J.-Q.; Yang, S.-D. Org. Lett. 2017, 19, 5434. (h) Magar, K. B. S.; Edison, T. N. J. I.; Lee, Y. R. Eur. J. Org. Chem. 2017, 2017, 7046. (i) Ghosh, B.; Biswas, A.; Chakraborty, S.; Samanta, R. Chem. Asian J. 2018, 13, 2388. (j) Jang, Y.-S.; Woźniak, Ł.; Pedroni, J.; Cramer, N. Angew. Chem. Int. Ed. 2018, 57, 12901. (k) Ghosh, B.; Samanta, R. Chem. Commun. 2019, 55, 6886. (l) Li, X.; Wang, J.; Xie, X.; Dai, W.; Han, X.; Chen, K.; Liu, H. Chem. Commun. 2020, 56, 3441.

(5) (a) Kitamura, M.; Otsuka, K.; Takahashi, S.; Okauchi, T. Tetrahedron Lett. 2017, 58, 3508. (b) Othman, D. I. A.; Otsuka, K.; Takahashi, S.; Selim, K. B.; El-Sayed, M. A.; Tantawy, A. S.; Okauchi, T.; Kitamura, M. Synlett 2018, 29, 457.

(6) Kitamura, M.; Kisanuki, M.; Sakata, R.; Okauchi, T. Chem. Lett. 2011, 40, 1129.

(7) (a) Kitamura, M.; Sakata, R.; Okauchi, T. Tetrahedron Lett. 2011, 52, 1931. (b) Kitamura, M.; Kisanuki, M.; Okauchi, T. Eur. J. Org. Chem. 2012, 2012, 905. (c) Kitamura, M.; Araki, K.; Matsuzaki, H.; Okauchi, T. Eur. J. Org. Chem. 2013, 2013, 5045. (d) Kitamura, M.; Kisanuki, M.; Kanemura, K.; Okauchi, T. Org. Lett. 2014, 16, 1554. (e) Baral, E. R.; Lee, Y. R.; Kim, S. H.; Wee, Y.-J. Synthesis 2016, 48, 579.

(8) (a) Ashkenazi, N.; Vigalok, A.; Parthiban, S.; Ben-David, Y.; Shimon, L. J. W.; Martin, J. M. L.; Milstein, D. J. Am. Chem. Soc. 2000, 122,

8797. (b) Dauth, A.; Gellrich, U.; Diskin-Posner, Y.; Ben-David, Y.; Milstein, D. J. Am. Chem. Soc. 2017, 139, 2799.
(9) Wu, K.; Cao, B.; Zhou, C.-Y.; Che, C.-M. Chem. Eur. J. 2018, 24, 4815.
(10) Wang, H.-X.; Wan, Q.; Wu, K.; Low, K.-H.; Yang, C.; Zhou, C.-Y.; Huang, J.-S.; Che, C.-M. J. Am. Chem. Soc. 2019, 141, 9027.
(11) Wang, H.-X.; Richard, Y.; Wan, Q.; Zhou, C.-Y.; Che, C.-M. Angew. Chem. Int. Ed. 2020, 59, 1845.
(12) (a) Collman, J. P.; Brothers, P. J.; McElwee-White, L.; Rose, E.; Wright, L. J. J. Am. Chem. Soc. 1985, 107, 4570. (b) Collman, J. P.; Rose, E.; Venburg, G. D. J. Chem. Soc. Chem. Commun. 1993, 934. (c) Galardon, E.; Maux, P. L.; Toupet, L.; Simonneaux, G. Organometallics 1998, 17, 565. (d) Che, C.-M.; Huang, J.-S.; Lee, F.-W.; Li, Y.; Lai, T.-S.; Kwong, H.-L.; Teng, P.-F.; Lee, W.-S.; Lo, W.-C.; Peng, S.-M.; Zhou, Z.-Y. J. Am. Chem. Soc. 2001, 123, 4119. (e) Che, C.-M.; Huang, J.-S. Coord. Chem. Rev. 2002, 231, 151. (f) Li, Y.; Huang, J.-S.; Xu, G.-B.; Zhu, N.; Zhou, Z.-Y.; Che, C.-M.; Wong, K.-Y. Chem. Eur. J. 2004, 10, 3486. (g) Che, C.-M.; Ho, C.-M.; Huang, J.-S. Coord. Chem. Rev. 2007, 251, 2145. (h) Le Maux, P.; Roisnel, T.; Nicolas, I.; Simonneaux, G. Organometallics 2008, 27, 3037. (i) Deng, Q.-H.; Chen, J.; Huang, J.-S.; Chui, S. S.-Y.; Zhu, N.; Li, G.-Y.; Che, C.-M. Chem. Eur. J. 2009, 15, 10707. (j) Wang, H.-X.; Wan, Q.; Low, K.-H.; Zhou, C.-Y.; Huang, J.-S.; Zhang, J.-L.; Che, C.-M. Chem. Sci. 2020, 11, 2243.
(13) (a) Reddy, A. R.; Guo, Z.; Siu, F.-M.; Lok, C.-N.; Liu, F.; Yeung, K.-C.; Zhou, C.-Y.; Che, C.-M. Org. Biomol. Chem. 2012, 10, 9165. (b) Reddy, A. R.; Zhou, C.-Y.; Che, C.-M. Org. Lett. 2014, 16, 1048. (c) Wu, K.; Zhou, C.-Y.; Che, C.-M. Org. Lett. 2018, 21, 85.
(14) (a) Li, Y.; Huang, J.-S.; Zhou, Z.-Y.; Che, C.-M.; You, X.-Z. J. Am. Chem. Soc. 2002, 124, 13185. (b) Li, Y.; Huang, J.-S.; Zhou, Z.-Y.; Che, C.-M. J. Am. Chem. Soc. 2001, 123, 4843.
(15) Miller, J. S.; Min, K. S. Angew. Chem. Int. Ed. 2009, 48, 262.
(16) (a) Kadish, K. M.; Deng, Y. J.; Yao, C.-L.; Anderson, J. E. Organometallics 1988, 7, 1979. (b) Palmer, J. H.; Day, M. W.; Wilson, A. D.; Henling, L. M.; Gross, Z.; Gray, H. B. J. Am. Chem. Soc. 2008, 130, 7786.
(17) For reviews on metal carbene radical reactivity, see: (a) Dzik, W. I.; Zhang, X. P.; de Bruin, B., Inorg. Chem. 2011, 50, 9896. (b) van Leest, N. P.; Epping, R. F. J.; van Vliet, K. M.; Lankelma, M.; van den Heuvel, E. J.; Heijtbrink, N.; Broersen, R.; de Bruin, B. In Advances in Organometallic Chemistry, Vol. 70; Pérez, P. J.; Stone, F. G. A.; West, R., Eds. Academic Press: 2018, 71.
(18) Kornecki, K. P.; Briones, J. F.; Boyarskikh, V.; Fullilove, F.; Autschbach, J.; Schrote, K. E.; Lancaster, K. M.; Davies, H. M. L.; Berry, J. F. Science 2013, 342, 351.
(19) Wu, K; Wu, L.-L.; Zhou, C.-Y.; Che, C.-M. Angew. Chem. Int. Ed. 2020, DOI: 10.1002/anie.202006542.
(20) Öfele, K.; Tosh, E.; Taubmann, C.; Herrmann, W. A. Chem. Rev. 2009, 109, 3408.

Biosketches

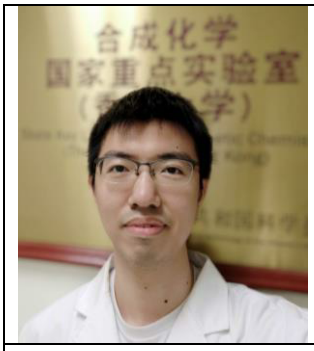

Dr. Hai-Xu Wang received his B.Sc. degree (first-class honour) in 2014 from the Hong Kong Polytechnic University and conducted undergraduate research with Prof. Wing-Yiu Yu on Pd-catalyzed C–H functionalization reactions. He then pursued graduate study on metal-carbene chemistry in the University of Hong Kong under the supervision of Prof. Chi-Ming Che, and obtained his Ph.D. degree in 2019. His current research interests include base metal catalysis and other new synthetic methodologies with an underlying focus on mechanistic understanding.

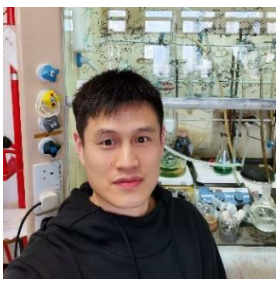

Mr. Kai Wu received his M.S. degree in 2014 from Zhejiang Sci-Tech University and conducted research with Prof. Yi-Feng Han on design and synthesis of novel BODIPY-based fluorescence probes. After working as a Research Scientist 1 at WuXi AppTec for about 1 year, he joined Prof. Chi-Ming Che's group at The University of Hong Kong to pursue his Ph.D. degree. His current research interest focuses on metal-carbene C-H functionalization reactions and other new synthetic methodologies based on diazo compound.

Prof. Chi-Ming Che received his Ph.D. degree in 1982 from The University of Hong Kong (HKU) under the supervision of Professor Chung-Kwong Poon. From 1980 to 1983, he studied at the California Institute of Technology under the supervision of Professor Harry B. Gray. Thereafter, he returned back to HKU and was promoted to Chair Professor in Chemistry in 1992. He was named as Dr Hui Wai-Haan Chair of Chemistry in 1999 and Zhou Guangzhao Professor in Natural Sciences in 2016. Professor Che was elected to member of the Chinese Academy of Sciences in 1995, received the prestigious First-Class Prize of State Natural Science Award from China in 2007, elected as Foreign Associate of National Academy of Sciences, USA in 2013, received the 2016 Huang Yao-Zeng Organometallic Chemistry Award of the Chinese Chemical Society – Lifetime Achievement Award in 2016 and Ryoji Noyori ACES Award in 2016. His research interests include inorganic and organic synthesis, reactive metal-ligand multiple bonds, metal-catalyzed organic transformations, organometallic and inorganic photochemistry, luminescent materials, and chemical biology of inorganic medicines. He has published over 1000 papers in leading chemistry journals with an h-index of 116.